

RESEARCH LETTER

10.1002/2016GL070052

Key Points:

- Aerosol optical depth has decreased due to reduced sulfur dioxide emissions
- Reduced diffuse radiation decreased cumulative gross primary productivity by 0.5 Pg C during 1995–2013
- CESM trends agree with upscaled flux tower results within 20%

Supporting Information:

- Supporting Information S1

Correspondence to:

G. Keppel-Aleks,
gkeppela@umich.edu

Citation:

Keppel-Aleks, G., and R. A. Washenfelder (2016), The effect of atmospheric sulfate reductions on diffuse radiation and photosynthesis in the United States during 1995–2013, *Geophys. Res. Lett.*, *43*, 9984–9993, doi:10.1002/2016GL070052.

Received 15 JUN 2016

Accepted 7 SEP 2016

Accepted article online 10 SEP 2016

Published online 28 SEP 2016

©2016. The Authors.

This is an open access article under the terms of the Creative Commons Attribution-NonCommercial-NoDerivs License, which permits use and distribution in any medium, provided the original work is properly cited, the use is non-commercial and no modifications or adaptations are made.

The effect of atmospheric sulfate reductions on diffuse radiation and photosynthesis in the United States during 1995–2013

G. Keppel-Aleks¹ and R. A. Washenfelder^{2,3}

¹Department of Climate and Space Sciences and Engineering, University of Michigan, Ann Arbor, Michigan, USA,

²Cooperative Institute for Research in Environmental Sciences, University of Colorado Boulder, Boulder, Colorado, USA,

³Chemical Sciences Division, Earth System Research Laboratory, National Oceanic and Atmospheric Administration, Boulder, Colorado, USA

Abstract Aerosol optical depth (AOD) has been shown to influence the global carbon sink by increasing the fraction of diffuse light, which increases photosynthesis over a greater fraction of the vegetated canopy. Between 1995 and 2013, U.S. SO₂ emissions declined by over 70%, coinciding with observed AOD reductions of $3.0 \pm 0.6\% \text{ yr}^{-1}$ over the eastern U.S. In the Community Earth System Model (CESM), these trends cause diffuse light to decrease regionally by almost $0.6\% \text{ yr}^{-1}$, leading to declines in gross primary production (GPP) of $0.07\% \text{ yr}^{-1}$. Integrated over the analysis period and domain, this represents 0.5 Pg C of omitted GPP. A separate upscaling calculation that used published relationships between GPP and diffuse light agreed with the CESM model results within 20%. The agreement between simulated and data-constrained upscaling results strongly suggests that anthropogenic sulfate trends have a small impact on carbon uptake in temperate forests due to scattered light.

1. Introduction

Terrestrial ecosystems affect climate by regulating fluxes of energy, water, and carbon. Currently, global ecosystems are a sink for anthropogenic CO₂ because gross primary productivity (GPP; the rate of photosynthesis) exceeds ecosystem respiration when integrated over an annual cycle. In order to quantify and predict the magnitude of the terrestrial carbon sink, it is necessary to understand the complex factors that affect GPP. On a global scale, temperature [Cox *et al.*, 2013; Wang *et al.*, 2013], growing season length [Piao *et al.*, 2007], atmospheric CO₂ concentrations [Schimel *et al.*, 2015; Zhu *et al.*, 2016], and water balance [Gatti *et al.*, 2014; Nemani *et al.*, 2002] all play important roles in controlling GPP variability.

Natural and anthropogenic aerosols may also affect the terrestrial carbon sink by scattering photosynthetically active radiation (PAR) to increase diffuse light and decrease direct light at the surface [Mahowald, 2011]. Diffuse light illuminates a greater fraction of the canopy, which increases light use efficiency and terrestrial carbon uptake [e.g., Alton *et al.*, 2007; Dengel and Grace, 2010; Oliphant *et al.*, 2011]. A number of observational studies have found positive correlations between diffuse radiation and photosynthesis [see Kanniah *et al.*, 2012, and references therein]. Modeling studies have similarly suggested that this effect may be a significant driver of the global terrestrial carbon sink. For example, Mercado *et al.* [2009] concluded that diffuse light increased the strength of the land sink by one quarter from 1960 to 1999 and Chen and Zhuang [2014] reported that present-day aerosol is responsible globally for 5 Pg C yr⁻¹ of GPP and 4 Pg C yr⁻¹ of net ecosystem production (which exceeds the present-day land sink of ~3 Pg C yr⁻¹) when compared to an aerosol-free control run.

The links among aerosol, scattered light, and photosynthesis indicate that changes in aerosol abundance can affect the magnitude of the land carbon sink. Anthropogenic primary and secondary aerosol make a large contribution to global aerosol mass [Boucher *et al.*, 2013]. One of the major sources of anthropogenic aerosol is sulfur dioxide (SO₂) from coal-fired power plants and industrial processes, which is oxidized in the atmosphere to form sulfate (SO₄²⁻) aerosol. As a result of the 1990 Clean Air Act Amendments in the United States, SO₂ emissions decreased 60% [Hand *et al.*, 2012], causing rapid changes in aerosol mass. For example, from 2001 to 2013 in the southeastern U.S., sulfate aerosol mass at surface sites decreased by $4.5(\pm 0.9)\% \text{ yr}^{-1}$ and aerosol optical depth (AOD) at 555 nm decreased by $3.5\% \text{ yr}^{-1}$ [Attwood *et al.*, 2014]. As aerosol

extinction decreases, both total radiation and the fraction of direct solar radiation at the surface increase [Goldstein *et al.*, 2009; Ramanathan and Feng, 2009], with potential effects on photosynthesis.

In this study, we examine the effect of decreasing SO₂ emissions on GPP within the eastern United States. We focus on the eastern U.S. because (1) rapid decreases in SO₂ emissions over the past two decades create an opportunity to examine the effects of reduced SO₄ mass and aerosol optical depth; (2) SO₂ emissions in the United States have been well quantified; and (3) carbon fluxes within temperate ecosystems in the eastern United States have been well observed. We use accurate SO₂ emission data for 1995–2013 in the Community Earth System Model (CESM) to determine trends in AOD, surface radiation, and photosynthesis. We evaluate modeled AOD against satellite data and compare the modeled photosynthetic response to an upscaled calculation constrained by published relationships between diffuse radiation and photosynthesis. By comparing simulations with a mechanistic land model and an empirically constrained upscaling, we show that even large reductions in aerosol precursor emissions have only modest impacts on regional GPP.

2. Methods

2.1. Approach 1: Community Earth System Model (CESM) Determination of GPP

We simulated the impact of decreases in SO₂ emissions from the United States on aerosol optical depth, solar radiation, and terrestrial carbon exchange using the CESM atmosphere and land models.

2.1.1. Sulfur Dioxide Emissions Inventory

We compiled an SO₂ emissions inventory for the United States based on Environmental Protection Agency (EPA) data from 1995 to 2013. The EPA requires the use of Continuous Emission Monitoring Systems (CEMS) to measure hourly emissions of SO₂ and NO_x for power plants and industrial sources regulated under the Acid Rain Program. This includes every unit that generates more than 25 MW of power and new units that generate less than 25 MW of power using fuel with sulfur content greater than 0.05% by weight [Burns *et al.*, 2011]. The CEMS data have been validated with 38 aircraft transects downwind of Texas power plants during 2000 and 2006, which showed an average agreement of $-0.7\% \pm 12.1\%$ for SO₂/CO₂ ratios and an absolute accuracy of $\sim 6\%$ for CEMS SO₂ data [Peischl *et al.*, 2010]. We assigned the CEMS SO₂ sources to a 1° latitude × 1° longitude grid by month and year for 1995–2013 (Figures 1a and 1b). CEMS monitoring accounted for 66–80% of U.S. SO₂ sources in the categories of “stationary fuel combustion” and “industrial and other processes” during 1995–2013 [US 2015], and the data were scaled to account for the unmonitored sources in these two categories, with the assumption that their geographical distribution is the same. We used the standard SO₂ emissions inventory for year 2000 for all sources outside the U.S., as well as for mobile sources, wildfires, agricultural burning, volcanoes, and domestic emissions within the U.S. [Lamarque *et al.*, 2010]. Chemical emissions of other species, including NO_x, were unchanged from the standard year 2000 model input [Lamarque *et al.*, 2010].

2.1.2. Chemistry, Aerosol, and Land Models

We simulated the effect of SO₂ emission reductions on photosynthesis using a two-step process. First, we used the Community Atmosphere Model (CAM4.0) [Neale *et al.*, 2013] to simulate changes in diffuse and direct light as a consequence of SO₂ emissions reductions. Second, we used these radiation fields as input conditions to the Community Land Model (CLM4.5) [Lawrence *et al.*, 2012, 2011] to simulate their impacts on land carbon uptake.

CAM4.0 was run at a horizontal resolution of $1.9^\circ \times 2.5^\circ$ using a finite volume dynamical core with 26 vertical levels. Ocean boundary conditions for this run were provided from a merged product that combines Hadley Centre sea ice and surface temperature data with higher resolution NOAA optimum interpolation analysis [Hurrell *et al.*, 2008]. Within CAM4.0, we used the Bulk Aerosol Model (BAM) to calculate gas- and aqueous-phase oxidation of SO₂ to sulfate and its contribution to aerosol mass [Lamarque *et al.*, 2012]. BAM efficiently computes the total mass of aerosol using an assumed lognormal size distribution. The optical properties of sulfate aerosol are computed in 14 shortwave bands (from 0.2 to 12.2 μm) using the Rapid Radiative Transfer Model (RRTMG) [Mlawer *et al.*, 1997]. RRTMG distinguishes between direct and diffuse solar radiation by parameterizing the scattering phase function using the Henyey-Greenstein approximation. These optical properties influence diffuse and direct radiation at visible (0.2–0.7 μm) and near-infrared (>0.7 μm) wavelengths. To isolate the impact of SO₂ emissions reductions, other

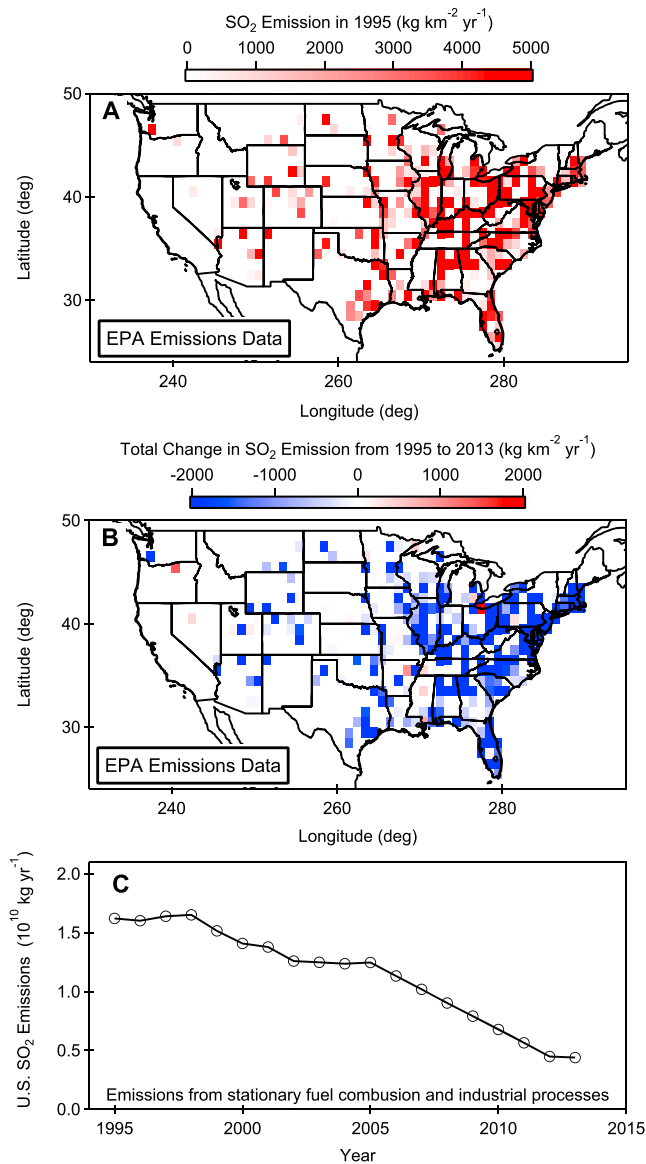


Figure 1. SO₂ emissions from EPA CEMS data, scaled to include “stationary fuel combustion” and “industrial and other process” sources not monitored by CEMS (see text). (a) SO₂ emissions for 1995. (b) Difference in SO₂ emissions between 1995 and 2013. (c) Total U.S. SO₂ emissions for 1995–2013.

use by sunlit and shaded leaves [Bonan *et al.*, 2011], and the maximum rate of carboxylation, $V_{c,max}$ is calculated separately for sunlit and shaded leaves because nitrogen allocation decreases with depth in the canopy. For our simulations, leaf area index in CLM4.5 was fixed according to satellite-derived phenology.

We spun-up CLM4.5 with the CRUNCEP temperature, precipitation, wind data, and year 1995 CAM4.0 diffuse and direct radiation until photosynthesis achieved steady state after approximately 200 years. We then used the archived radiation fields from CAM4.0/BAM to simulate the effect of decreasing diffuse fraction on monthly mean photosynthesis in CLM4.5 over 19 years. We assessed correlations between growing season (June, July, August; JJA) photosynthesis and radiation fields, but also calculated the annually integrated gross carbon uptake for our analysis. We calculated absolute trends in the data using ordinary least squares regression and calculated relative trends (% yr⁻¹) using ordinary least squares regression for the natural log of the variable.

precursor emissions and greenhouse gas mole fractions were fixed at their year 2000 values. We ran the model for 19 years (1995–2013) and archived four radiation values (direct and diffuse radiation at visible and near-infrared wavelengths) at hourly resolution. We also archived AOD values for the 442–625 nm wavelength band.

The direct and diffuse visible and near-infrared radiation values from a single ensemble member were subsequently used as boundary conditions within CLM4.5 with reanalysis meteorology derived from Hadley Centre Climate Research Unit observations and National Centers for Environmental Prediction (CRUNCEP) reanalysis data. We did not run a coupled land-atmosphere simulation due to coupling problems between CAM4 and CLM4.5 that have since been resolved in CAM5 (D. Lawrence, personal communication, 2015), but our approach provides realistic boundary conditions to the land model. We used annually repeating meteorological data to isolate the impact of diffuse light from interannual climate variability. CLM4.5 simulates biogeophysical interactions between the land surface and the atmosphere, including sensible and latent heat fluxes [Lawrence *et al.*, 2011]. Photosynthesis is simulated within CLM4.5 using a modified Ball-Berry model to relate stomatal conductance to net assimilation [Lawrence *et al.*, 2011]. Compared to prior versions, CLM4.5 better represents light

2.2. Approach 2: Flux Tower Upscaling to Determine GPP

Given the large range of model predictions for GPP-diffuse light correlations, we evaluated the accuracy of CESM GPP trends against an upscaling calculation constrained by eddy covariance flux observations. We used published relationships between radiation and GPP for different ecosystem types [Cheng *et al.*, 2015] and matched these to 17 land cover types determined from satellite observations (Table S1 in the supporting information). Finally, we used direct and diffuse visible radiation from CAM4.0/BAM to calculate trends in photosynthesis during 1995–2013. This approach allowed us to make a simple calculation of the trend in photosynthesis, independent of the biogeophysics represented in the CLM4.5 model.

2.2.1. Land Cover and Radiation

Land cover type was taken from the Moderate Resolution Imaging Spectroradiometer (MODIS) L3 annual data (MCD12C1) with 0.05° resolution [Friedl *et al.*, 2010]. We used the International Geosphere-Biosphere Programme (IGBP) classification scheme, which includes 11 natural vegetation classes, three developed and mosaicked land classes, and three nonvegetated land classes [Loveland and Belward, 1997]. We neglected land cover changes in the U.S. over the study period and used the 2001 land cover assignments for all years.

Direct and diffuse visible radiation were taken from CAM4.0/BAM, as described in section 2.1.2. We scaled CESM visible radiation (0.2–0.7 μm) by 0.94 to match PAR (typically defined as 0.4–0.7 μm), based on observed ratios [Gueymard, 1989; Papaioannou *et al.*, 1993].

2.2.2. Published Relationships Between GPP, Direct, and Diffuse Radiation

Cheng *et al.* [2015] used data from AmeriFlux towers in temperate forests and agricultural sites to calculate site-specific relationships between GPP, PAR_{direct}, and PAR_{diffuse}. We represented GPP as

$$\text{GPP} = \frac{\alpha\gamma\text{PAR}_{\text{direct}}}{\gamma + \alpha\text{PAR}_{\text{direct}}} + \beta_1\text{PAR}_{\text{diffuse}} \quad (1)$$

where α is the canopy quantum efficiency, γ is the canopy photosynthetic potential, and β_1 is the slope of the relationship between photosynthesis and diffuse light, accounting for confounding impacts of direct light, air temperature, and vapor pressure deficit. We use the reported parameters for α , β_1 , and γ from Cheng *et al.* [2015] averaged for solar zenith angles less than 60°. We matched the four measurement locations (shown as open green circles in Figure 3) from Cheng *et al.* [2015] to the 17 land cover types from the IGBP classification scheme. Further information and α , β_1 , and γ values are given in Table S1 of the supporting information.

2.2.3. Error Estimation

The uncertainty in the flux tower upscaling was calculated analytically from equation (1) for each 1.9° × 2.5° grid cell. The variability in visible direct and diffuse radiation modeled by CESM was determined from three CAM4.0/BAM model repetitions with identical emissions but different patterns of climate variability during the 19 year runs due to the sensitivity of the atmosphere to initial conditions. Interannual climate variability affects the chemical conversion of SO₂ to sulfate aerosol, the transport of both SO₂ and sulfate from source regions, and the influence of AOD on diffuse and direct radiation because it is modulated by clouds. The average uncertainty in α , β_1 , and γ values were estimated to be 16%, 16%, and 2%, respectively (S. J. Cheng, personal communication, 2016). The uncertainty in MODIS IGBP land cover classifications was neglected. The average calculated uncertainty in the flux tower upscaling for the eastern U.S. was 27%.

2.3. Other Data Sets

2.3.1. Satellite Measurement of Aerosol Optical Depth for Model Evaluation

The trends and magnitude of AOD at 550 nm from the CAM4.0 model were validated using Multiangle Imaging Spectroradiometer (MISR) L3 data at 555 nm with 0.5 deg resolution [Kahn *et al.*, 2009] for summer periods (JJA) during 2001–2013. AOD trends in the eastern United States during 2001–2013 [−0.003 to −0.015 yr^{−1}; Attwood *et al.*, 2014] were much greater than the MISR uncertainty (±0.0003 yr^{−1}) [Zhang and Reid, 2010].

3. Results and Discussion

3.1. Trends in Sulfur Dioxide and Aerosol Optical Depth

EPA emissions data indicate that total SO₂ emissions from stationary fuel combustion and industrial processes for the continental United States declined by more than 70% between 1995 and 2013 (Figure 1c), from

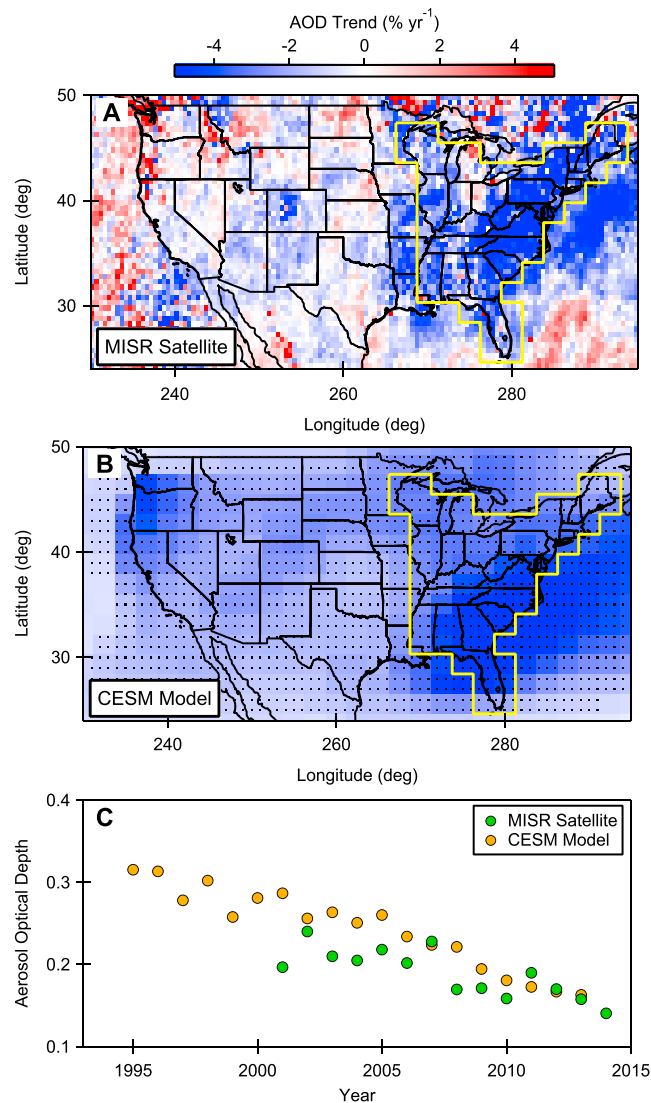


Figure 2. Annual trends in AOD from 2001 to 2013 for summer (JJA) from (a) MISR Level 3 at 555 nm; (b) CESM model at 555 nm. (c) AOD values for MISR and CESM, showing JJA average for the eastern U.S., as defined by the yellow outline in Figures 2a and 2b. Stipples in this figure indicate p values ≤ 0.05 .

the CAM4.0/BAM model is able to accurately simulate aerosol extinction based on SO_2 emissions and further suggests that CAM4.0 reasonably represents direct and diffuse radiation trends.

3.2. Trend in Diffuse Radiation and Photosynthesis From CESM Model

The CESM model simulates an absolute decline in diffuse radiation of $0.2\text{--}0.3 \text{ W m}^{-2} \text{ yr}^{-1}$ during JJA from 1995 to 2013 over the eastern U.S., equivalent to a relative trend of $-0.6 \pm 0.2\% \text{ yr}^{-1}$ (Figure 3a). Diffuse and direct radiation covary, and CESM simulates an increase in direct radiation of $0.3 \pm 0.2\% \text{ yr}^{-1}$ for the same time period, resulting in a total visible radiation increase of $0.1 \pm 0.2\% \text{ yr}^{-1}$.

When these radiation values are input as boundary conditions to the Community Land Model (CLM4.5) with CRUNCEP reanalysis meteorology, the simulated trend is $-0.11 \pm 0.04\% \text{ yr}^{-1}$ for JJA GPP and $-0.07 \pm 0.03\% \text{ yr}^{-1}$ for annual GPP from 1995–2013 over the eastern U.S. (Figure 3b). The absolute decline was $4.5 \pm 2.0 \text{ Tg C y}^{-2}$. Modeled GPP for a control simulation with diffuse and direct radiation fields fixed at their 1995 values does not show significant trends (Figure S1). Over the 19 years of our study, these trends

$1.6 \times 10^{10} \text{ kg yr}^{-1}$ in 1995 to $0.4 \times 10^{10} \text{ kg yr}^{-1}$ in 2013. The largest absolute changes occurred in the eastern and southeastern U.S. (Figure 1b) and can be attributed to emission regulations implemented under the 1990 Clean Air Act and its amendments (Figure 1c).

AOD likewise decreased over the eastern and southeastern U.S. during this time period. Both the MISR satellite and the CESM model simulated AOD decreases of several percent per year across the eastern U.S., and the largest decreases were geographically coincident with decreased SO_2 emissions (Figure 2). During the period from 2001 to 2013, when both MISR and CESM data are available, MISR measured an average AOD trend of $-3.0 \pm 0.6\% \text{ yr}^{-1}$ with a mean AOD of 0.19 over the eastern U.S. (yellow outlined area in Figures 2a and 2b). For the same area and time period, the CESM model simulated an average AOD trend of $-4.9 \pm 0.3\% \text{ yr}^{-1}$ with a mean AOD of 0.22, using an accurate SO_2 emissions inventory and other emissions held constant at their year 2000 values. In addition to decreasing aerosol SO_4 mass, the MISR measurements are influenced by smaller trends due to decreasing aerosol nitrate, elemental carbon, and organic carbon mass [Hand et al., 2014], so we do not expect absolute agreement with the CESM model. However, the fact that CESM simulates both absolute values and trends in AOD that are similar to the MISR observations indicates that

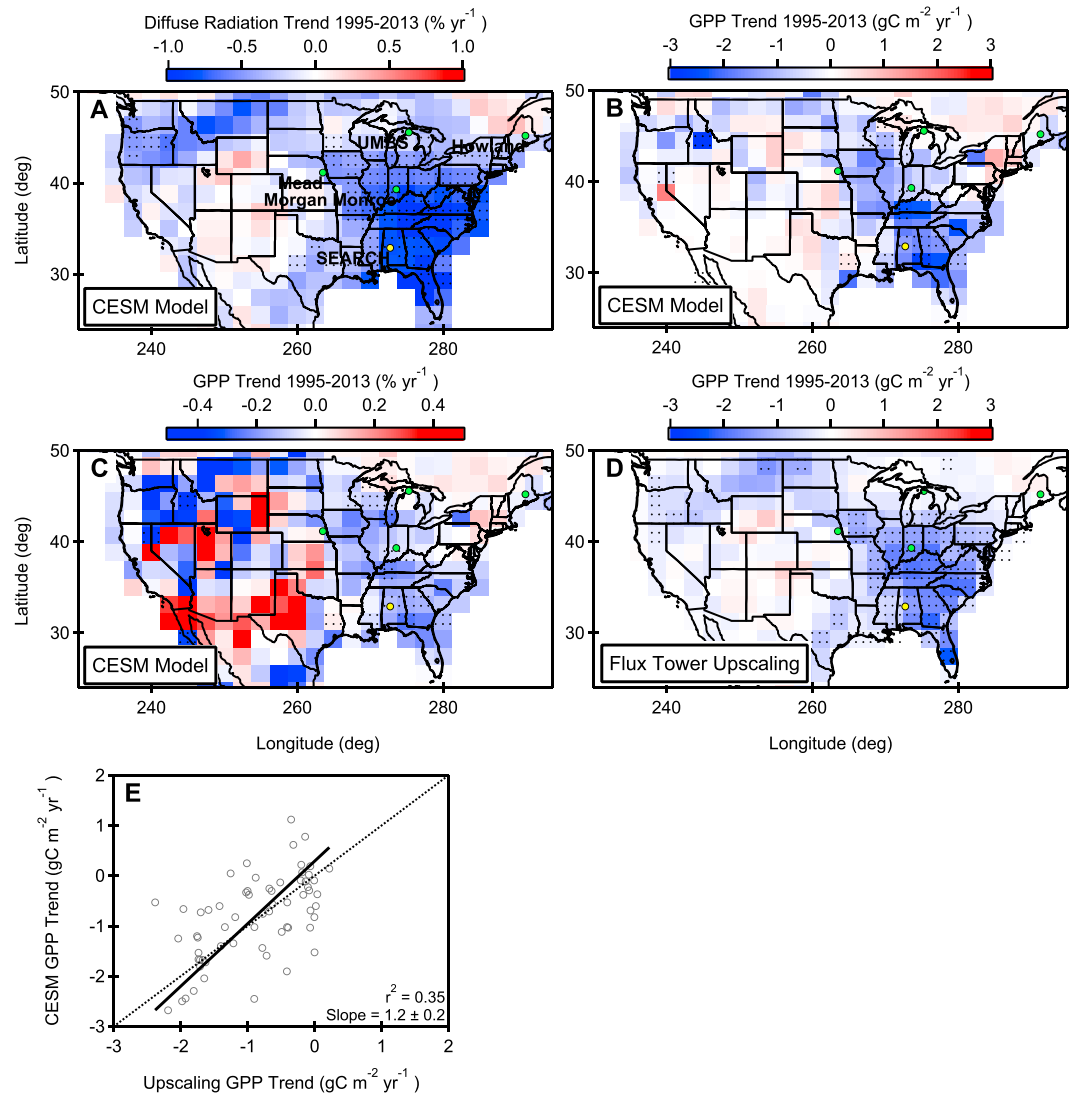


Figure 3. Annual trends from 1995 to 2013 for summer (JJA) for (a) modeled diffuse radiation (FSDSVI) from CEM; (b) modeled GPP trend from CEM in absolute units; (c) modeled GPP trend from CEM in % yr⁻¹; (d) calculated GPP trend from flux tower upscaling in absolute units, using visible direct and visible diffuse radiation from CEM model, MODIS landcover, and relationships between GPP, visible direction, and visible diffuse reported by *Cheng et al.* [2015]. Stipples in this figure indicate p values ≤ 0.05 . (e) Correlation plot showing GPP trends from the CEM model and flux tower upscaling for 1995–2013. The slope (solid black line) is 1.2 ± 0.2 with $r^2 = 0.35$, and the one-to-one line (grey dotted line) is shown. In all panels, the open green circles show the flux tower sites from *Cheng et al.* [2015] used for the upscaling calculation, and the open yellow circle shows the Alabama SEARCH site.

represent a cumulative reduction in gross carbon uptake of $1.1 \pm 0.04\%$ over the eastern U.S., which is equivalent to about 0.5 Pg C of omitted photosynthesis due to reductions in SO₂ emissions relative to the control.

Differences in the GPP trend across the eastern U.S. were tied primarily to the magnitude of change in diffuse light. Because atmospheric variables were prescribed from CRUNCEP reanalysis, vegetation temperature increased by only 0.003 K yr^{-1} averaged over the eastern U.S., and trends at the grid cell level were not statistically significant at the 95% confidence level. Rather, the relative trend in photosynthesis was correlated with the magnitude of the diffuse light decrease. The southeastern U.S. (south of 40°N) saw both the largest trend in diffuse light and the largest relative trend in photosynthesis, about one third greater than the relative trend north of 40°N (Figures 3b and 3c). The grid cells with the largest trends contained plant functional types

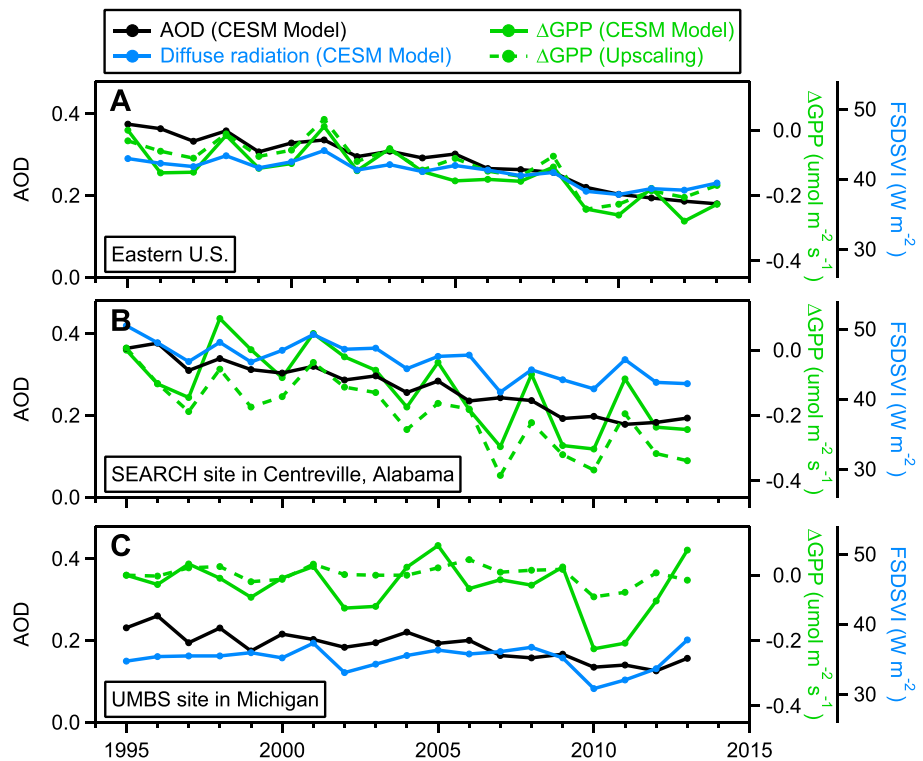


Figure 4. CESM modeled trends for AOD, diffuse radiation (FSDSVI), and GPP shown together with GPP determined from flux tower upscaling. Δ GPP is equal to $GPP - GPP_{1995}$ for each time series. Shown are (a) spatially averaged trends for the eastern U.S. (as defined by the yellow outline in Figure 2a); (b) the SEARCH site in Centreville, Alabama; and (c) the UMBS site, in Michigan.

in equal proportion to the entire domain, suggesting that vegetation distributions did not drive the spatial variability. Multiple linear regression did not show statistically significant differences for the diffuse light efficiency for different plant functional types, nor did it yield robust results for separating the influence of direct and diffuse light.

3.3. Trend in Photosynthesis From Flux Tower Upscaling

Figure 4 shows temporal trends in AOD, diffuse radiation, and GPP from the CESM model for the eastern U.S., together with the trend in GPP determined from the flux tower upscaling. Photosynthesis decreased on average by $-0.97 \pm 0.19 \text{ gC m}^{-2} \text{ yr}^{-1}$ over 19 years for the eastern U.S. (Figure 4a) when calculated using equation (1) with direct and diffuse visible radiation from CESM. The trends are geographically consistent with those from the CESM model (Figures 3b and 3d). For the eastern U.S., the trend predicted by CEMS is consistent with the flux tower upscaling within 9% (Table 1) while a scatterplot of the individual values shows

Table 1. Results for AOD, Diffuse PAR Response

Location	Lat, Lon (deg)	AOD Trend (% yr ⁻¹) 2001–2013		Diffuse Radiation Trend Modeled ^b		Diffuse PAR Response, β_1 ($\mu\text{mol CO}_2/\mu\text{mol Photon}$)		GPP Trend Upscaled ^b	GPP Trend Modeled ^b	
		Satellite ^a	Modeled ^b	($\text{W m}^{-2} \text{ yr}^{-1}$)	(% yr ⁻¹)	Published ^a	Modeled ^b	($\text{gC m}^{-2} \text{ yr}^{-1}$)	($\text{gC m}^{-2} \text{ yr}^{-1}$)	(% yr ⁻¹)
Eastern United States		-3.0	-4.9	-0.26	-0.6	NA	0.008	-0.97	-1.05	-0.11
SEARCH Centreville	32.903, 272.750	-4.6	-4.5	-0.37	-0.8	NA	0.001	-1.49	-1.40	-0.13
Howland Reference	45.207, 291.275	-3.0	-2.8	-0.08	-0.2	0.005	0.016	-0.11	-0.69	-0.08
Morgan Monroe	39.323, 273.587	-4.9	-3.1	-0.32	-0.7	0.009	0.000	-1.81	-0.73	-0.07
UMBS	45.559, 275.287	0.2	-3.2	-0.09	-0.3	0.011	0.008	-0.13	0.05	0.01

^aMISR.

^bThis work.

^cCheng et al. [2015], average of measurements at SZA < 60°.

consistency of 20% (Figure 3e). Figures 4b and 4c show model and flux tower upscaling results for the SEARCH site in Centreville, Alabama, where large reductions in AOD have occurred and the UMBS field site from *Cheng et al.* [2015] where more modest reductions in AOD have occurred.

4. Discussion and Conclusions

The CESM model predicts that the reduction in SO_2 emissions associated with the Clean Air Act Amendments has led to a $4.9 \pm 0.3\% \text{ yr}^{-1}$ change in AOD and a $3.0 \pm 0.6\% \text{ yr}^{-1}$ decline in diffuse radiation over the eastern U.S. between 1995 and 2013. We confirmed that simulation of AOD within CESM is in good agreement with MISR data for accurate historical SO_2 emissions. The impact of these changes on photosynthesis rates is confirmed by a simple flux tower upscaling calculation, which finds a consistent change in GPP over the eastern U.S. during the same period. These results suggest that the 1990 Clean Air Act Amendments, while improving air quality, had a small adverse impact on the U.S. carbon sink attributed to changes in direct and diffuse radiation.

Our results suggest that over a 19 year period, only 0.5 Pg C of GPP was omitted over the eastern U.S. despite significant changes in AOD and diffuse radiation. The small effect that we find in both CESM and the observationally constrained upscaling disagrees with recent results from *Strada and Unger* [2016], who report that anthropogenic aerosols enhance GPP by 5–8% annually over temperate ecosystems in eastern North America. Given that in our observationally constrained upscaling, the cumulative reduction in GPP was only 1%, their model result likely overestimates the influence of anthropogenic aerosol on GPP. Our results are more consistent with *Xia et al.* [2016], who used CLM4 to calculate that a $\sim 3 \text{ W m}^{-2}$ increase in diffuse light under a geoengineering scenario increases temperate forest photosynthesis by $\sim 0.07 \mu\text{mol C m}^{-2} \text{ s}^{-1}$, which agrees within a factor of 2 with our sensitivities from both CESM using CLM4.5 and the flux tower upscaling. The disparate results from different models underscore the importance of simulating quantities that can be compared to available observations. While our study considers only the impacts on photosynthesis, not net ecosystem exchange, we expect that the overall decrease to the land carbon sink is smaller than 0.5 Pg C integrated over 20 years due to respiration. Although this value only comprises the eastern U.S., the small change to photosynthesis resulting from a large change in sulfate aerosol does not support a substantial role for diffuse light impacts from anthropogenic aerosol as a driver of the historical land carbon sink [e.g., *Mercado et al.*, 2009]. Our results also suggest a minimal trade-off between future reductions in anthropogenic aerosol for improved air quality and their indirect impacts on the land carbon sink, at least in temperate ecosystems.

The decrease in SO_2 and NO_x ($\text{NO} + \text{NO}_2$) emissions due to the Clean Air Act Amendments are expected to have other impacts on carbon uptake that may enhance or offset the impacts of sulfate aerosol. Both SO_2 and NO_x contribute to acid deposition, which depletes nutrients such as calcium, magnesium, and potassium in the soil, and may contribute to tree mortality [*Driscoll et al.*, 2001]. Ozone is produced through photochemistry that requires NO_x , and its presence causes plant cellular damage through the degradation of stomata and reduced water use efficiency [*Holmes*, 2014; *Lombardozzi et al.*, 2015]. Decreased acid deposition and ozone concentration would both increase photosynthesis over the period from 1995 to 2013, counteracting the effect of reduced sulfate aerosol. Alternatively, decreased nitrogen deposition due to reduced NO_x emissions may decrease photosynthesis in nitrogen-limited ecosystems. This effect is likely small because eastern forests are only moderately sensitive to nitrogen additions [*Nadelhoffer et al.*, 1999], and chronic nitrogen additions may actually slow rates of carbon uptake [*Aber et al.*, 1989]. In contrast to our simulations, which were run with fixed climate, decreased AOD may lead to increased surface temperatures and reductions in photosynthesis. We designed our simulations to minimize this effect and to facilitate comparisons with the observational scale factors derived from *Cheng et al.* [2015]. Likewise, we have considered only the influence of sulfate aerosol on the aerosol direct effect and photosynthesis, independent from other factors which may have changed direct and diffuse radiation during the period from 1995 to 2013. Biogenic emissions that contribute to secondary organic aerosol may decrease as diffuse light decreases [*Strada and Unger*, 2016; *Wilton et al.*, 2011], although the magnitude is not well constrained and may be counteracted by covarying temperature increases [*Knohl and Baldocchi*, 2008]. Surface radiation data has shown increasing trends in both clear-sky total and diffuse shortwave radiation in the U.S., and this has been attributed to factors such as high-altitude cirrus or cloudiness [*Gan et al.*, 2014; *Long et al.*, 2009].

Uncertainty persists in the net impact anthropogenic activity has on ecosystem carbon uptake, and climate change predictions require accurate accounting of the radiative forcing of CO₂, as well as accurate accounting of numerous climate feedbacks that are driven by aerosol. Although we found that the effect of diffuse radiation on photosynthesis was small for the U.S., quantifying this interaction is an important step that should be considered for ecosystems globally. Future aerosol trends will likely be dominated by changes in anthropogenic emissions from China and other countries.

Acknowledgments

The research was supported in part by the Biogeochemistry–Climate Feedbacks Scientific Focus Area (SFA), which is sponsored by the Regional and Global Climate Modeling (RGCM) Program in the Climate and Environmental Sciences Division (CESD) of the Biological and Environmental Research Program in the U.S. Department of Energy Office of Science. We thank Greg Frost for advice about SO₂ emissions inventories. We thank Susan Cheng and Allison Steiner for helpful discussions on the flux tower data, and Mark Flanner for discussions about configuring CESM. Data are available from the authors upon request.

References

- Aber, J. D., K. J. Nadelhoffer, P. Steudler, and J. M. Melillo (1989), Nitrogen saturation in northern forest ecosystems, *BioScience*, *39*(6), 378–386, doi:10.2307/1311067.
- Alton, P. B., P. R. North, and S. O. Los (2007), The impact of diffuse sunlight on canopy light-use efficiency, gross photosynthetic product and net ecosystem exchange in three forest biomes, *Global Change Biol.*, *13*(4), 776–787.
- Attwood, A. R., et al. (2014), Trends in sulfate and organic aerosol mass in the Southeast U.S.: Impact on aerosol optical depth and radiative forcing, *Geophys. Res. Lett.*, *41*, 7701–7709, doi:10.1002/2014GL061669.
- Bonan, G. B., P. J. Lawrence, K. W. Oleson, S. Levis, M. Jung, M. Reichstein, D. M. Lawrence, and S. C. Swenson (2011), Improving canopy processes in the Community Land Model version 4 (CLM4) using global flux fields empirically inferred from FLUXNET data, *J. Geophys. Res.*, *116*, G02014, doi:10.1029/2010JG001593.
- Boucher, O., et al. (2013), Clouds and Aerosols, in *Climate Change 2013: The Physical Science Basis. Contribution of Working Group I to the Fifth Assessment Report of the Intergovernmental Panel on Climate Change*, edited by T. F. Stocker, D. Qin, G.-K. Plattner, M. Tignor, S. K. Allen, J. Boschung, A. Nauels, Y. Xia, V. Bex, and P. M. Midgley, Cambridge Univ. Press, U. K. and New York.
- Burns, D. A., J. A. Lynch, B. J. Cosby, M. E. Fenn, and J. S. Baron (2011), *National Acid Precitation Assessment Program Report to Congress 2011: An Integrated Assessment*, 114 pp., National Science and Technology Council, Washington, D. C.
- Chen, M., and Q. L. Zhuang (2014), Evaluating aerosol direct radiative effects on global terrestrial ecosystem carbon dynamics from 2003 to 2010, *Tellus B*, *66*, doi:10.3402/tellusb.v3466.21808.
- Cheng, S. J., G. Bohrer, A. L. Steiner, D. Y. Hollinger, A. Suyker, R. P. Phillips, and K. J. Nadelhoffer (2015), Variations in the influence of diffuse light on gross primary productivity in temperate ecosystems, *Agr. Forest Meteorol.*, *201*, 98–110.
- Cox, P. M., D. Pearson, B. B. Booth, P. Friedlingstein, C. Huntingford, C. D. Jones, and C. M. Luke (2013), Sensitivity of tropical carbon to climate change constrained by carbon dioxide variability, *Nature*, *494*(7437), 341–344.
- Dengel, S., and J. Grace (2010), Carbon dioxide exchange and canopy conductance of two coniferous forests under various sky conditions, *Oecologia*, *164*(3), 797–808.
- Driscoll, C. T., G. B. Lawrence, A. J. Bulger, T. J. Butler, C. S. Cronan, C. Eagar, K. F. Lambert, G. E. Likens, J. L. Stoddard, and K. C. Weathers (2001), Acidic deposition in the northeastern United States: Sources and inputs, ecosystem effects, and management strategies, *BioScience*, *51*(3), 180–198.
- Friedl, M. A., D. Sulla-Menashe, B. Tan, A. Schneider, N. Ramankutty, A. Sibley, and X. M. Huang (2010), MODIS collection 5 global land cover: Algorithm refinements and characterization of new datasets, *Remote Sens. Environ.*, *114*(1), 168–182.
- Gan, C. M., J. Pleim, R. Mathur, C. Hogrefe, C. N. Long, J. Xing, S. Roselle, and C. Wei (2014), Assessment of the effect of air pollution controls on trends in shortwave radiation over the United States from 1995 through 2010 from multiple observation networks, *Atmos. Chem. Phys.*, *14*(3), 1701–1715.
- Gatti, L. V., et al. (2014), Drought sensitivity of Amazonian carbon balance revealed by atmospheric measurements, *Nature*, *506*(7486), 76–80, doi:10.1038/nature12957.
- Goldstein, A. H., C. D. Koven, C. L. Heald, and I. Y. Fung (2009), Biogenic carbon and anthropogenic pollutants combine to form a cooling haze over the southeastern United States, *Proc. Natl. Acad. Sci. U.S.A.*, *106*(22), 8835–8840.
- Gueymard, C. (1989), A two-band model for the calculation of clear sky solar irradiance, illuminance, and photosynthetically active radiation at the Earth's surface, *Solar Energy*, *43*(5), 253–265, doi:10.1016/0038-092X(89)90113-8.
- Hand, J. L., B. A. Schichtel, W. C. Malm, and M. L. Pitchford (2012), Particulate sulfate ion concentration and SO₂ emission trends in the United States from the early 1990s through 2010, *Atmos. Chem. Phys.*, *12*(21), 10,353–10,365.
- Hand, J. L., B. A. Schichtel, W. C. Malm, S. Copeland, J. V. Molenar, N. Frank, and M. Pitchford (2014), Widespread reductions in haze across the United States from the early 1990s through 2011, *Atmos. Environ.*, *94*, 671–679.
- Holmes, C. D. (2014), Air pollution and forest water use, *Nature*, *507*(7491), E1–E2, doi:10.1038/nature13113.
- Hurrell, J. W., J. J. Hack, D. Shea, J. M. Caron, and J. Rosinski (2008), A new sea surface temperature and sea ice boundary dataset for the community atmosphere model, *J. Clim.*, *21*(19), 5145–5153, doi:10.1175/2008JCLI2292.1.
- Kahn, R. A., D. L. Nelson, M. J. Garay, R. C. Levy, M. A. Bull, D. J. Diner, J. V. Martonchik, S. R. Paradise, E. G. Hansen, and L. A. Remer (2009), MISR aerosol product attributes and statistical comparisons with MODIS, *IEEE T. Geosci. Remote*, *47*(12), 4095–4114.
- Kanniah, K. D., J. Beringer, P. North, and L. Hutley (2012), Control of atmospheric particles on diffuse radiation and terrestrial plant productivity: A review, *Prog. Phys. Geogr.*, *36*(2), 209–237.
- Knohl, A., and D. D. Baldocchi (2008), Effects of diffuse radiation on canopy gas exchange processes in a forest ecosystem, *J. Geophys. Res.*, *113*, G02023, doi:10.1029/2007JG000663.
- Lamarque, J. F., et al. (2010), Historical (1850–2000) gridded anthropogenic and biomass burning emissions of reactive gases and aerosols: methodology and application, *Atmos. Chem. Phys.*, *10*(15), 7017–7039.
- Lamarque, J. F., et al. (2012), CAM-chem: Description and evaluation of interactive atmospheric chemistry in the Community Earth System Model, *Geosci. Model Dev.*, *5*(2), 369–411.
- Lawrence, D. M., et al. (2011), Parameterization improvements and functional and structural advances in version 4 of the community land model, *J. Adv. Model. Earth Sy.*, *3*, 2011MS000045.
- Lawrence, D. M., K. W. Oleson, M. G. Flanner, C. G. Fletcher, P. J. Lawrence, S. Levis, S. C. Swenson, and G. B. Bonan (2012), The CCSM4 land simulation, 1850–2005: Assessment of surface climate and new capabilities, *J. Clim.*, *25*(7), 2240–2260.
- Lombardozi, D., S. Levis, G. Bonan, P. G. Hess, and J. P. Sparks (2015), The influence of chronic ozone exposure on global carbon and water cycles, *J. Clim.*, *28*(1), 292–305, doi:10.1175/JCLI-D-14-00223.1.
- Long, C. N., E. G. Dutton, J. A. Augustine, W. Wiscombe, M. Wild, S. A. McFarlane, and C. J. Flynn (2009), Significant decadal brightening of downwelling shortwave in the continental United States, *J. Geophys. Res.*, *114*, D00D06, doi:10.1029/2008JD011263.

- Loveland, T. R., and A. S. Belward (1997), The IGBP-DIS global 1 km land cover data set, DISCover: First results, *Int. J. Remote Sens.*, *18*(15), 3291–3295.
- Mahowald, N. (2011), Aerosol indirect effect on biogeochemical cycles and climate, *Science*, *334*(6057), 794–796.
- Mercado, L. M., N. Bellouin, S. Sitch, O. Boucher, C. Huntingford, M. Wild, and P. M. Cox (2009), Impact of changes in diffuse radiation on the global land carbon sink, *Nature*, *458*(7241), 1014–1017.
- Mlawer, E. J., S. J. Taubman, P. D. Brown, M. J. Iacono, and S. A. Clough (1997), Radiative transfer for inhomogeneous atmospheres: RRTM, a validated correlated-k model for the longwave, *J. Geophys. Res.*, *102*, P16663, doi:10.1029/97JD00237.
- Nadelhoffer, K. J., B. A. Emmett, P. Gundersen, O. J. Kjonaas, C. J. Koopmans, P. Schleppi, A. Tietema, and R. F. Wright (1999), Nitrogen deposition makes a minor contribution to carbon sequestration in temperate forests, *Nature*, *398*(6723), 145–148.
- Neale, R. B., J. Richter, S. Park, P. H. Lauritzen, S. J. Vavrus, P. J. Rasch, and M. H. Zhang (2013), The mean climate of the Community Atmosphere Model (CAM4) in forced SST and fully coupled experiments, *J. Clim.*, *26*(14), 5150–5168.
- Nemani, R., M. White, P. Thornton, K. Nishida, S. Reddy, J. Jenkins, and S. Running (2002), Recent trends in hydrologic balance have enhanced the terrestrial carbon sink in the United States, *Geophys. Res. Lett.*, *29*(10), 106-1–106-4, doi:10.1029/2002GL014867.
- Olyphant, A. J., D. Dragoni, B. Deng, C. S. B. Grimmond, H. P. Schmid, and S. L. Scott (2011), The role of sky conditions on gross primary production in a mixed deciduous forest, *Agr. Forest Meteorol.*, *151*(7), 781–791.
- Papaioannou, G., N. Papanikolaou, and D. Retalis (1993), Relationships of photosynthetically active radiation and shortwave irradiance, *Theor. Appl. Climatol.*, *48*(1), 23–27, doi:10.1007/BF00864910.
- Peischl, J., et al. (2010), A top-down analysis of emissions from selected Texas power plants during TexAQ5 2000 and 2006, *J. Geophys. Res.*, *115*, D16303, doi:10.1029/2009JD013527.
- Piao, S., P. Friedlingstein, P. Ciais, N. Viovy, and J. Demarty (2007), Growing season extension and its impact on terrestrial carbon cycle in the Northern Hemisphere over the past 2 decades, *Global Biogeochem. Cycles*, *21*, GB3018, doi:10.1029/2006GB002888.
- Ramanathan, V., and Y. Feng (2009), Air pollution, greenhouse gases and climate change: Global and regional perspectives, *Atmos. Environ.*, *43*, 37–50.
- Schimel, D., B. B. Stephens, and J. B. Fisher (2015), Effect of increasing CO₂ on the terrestrial carbon cycle, *Proc. Natl. Acad. Sci. U.S.A.*, *112*(2), 436–441.
- Strada, S., and N. Unger (2016), Potential sensitivity of photosynthesis and isoprene emission to direct radiative effects of atmospheric aerosol pollution, *Atmos. Chem. Phys.*, *16*(7), 4213–4234, doi:10.5194/acp-16-4213-2016.
- Wang, W., P. Ciais, R. R. Nemani, J. G. Canadell, S. Piao, S. Sitch, M. A. White, H. Hashimoto, C. Milesi, and R. B. Myneni (2013), Variations in atmospheric CO₂ growth rates coupled with tropical temperature, *Proc. Natl. Acad. Sci. U.S.A.*, *110*(32), 13,061–13,066.
- Wilton, D. J., C. N. Hewitt, and D. J. Beerling (2011), Simulated effects of changes in direct and diffuse radiation on canopy scale isoprene emissions from vegetation following volcanic eruptions, *Atmos. Chem. Phys.*, *11*(22), 11,723–11,731, doi:10.5194/acp-11-11723-2011.
- Xia, L., A. Robock, S. Tilmes, and R. R. Neely Iii (2016), Stratospheric sulfate geoengineering could enhance the terrestrial photosynthesis rate, *Atmos. Chem. Phys.*, *16*(3), 1479–1489, doi:10.5194/acp-16-1479-2016.
- Zhang, J., and J. S. Reid (2010), A decadal regional and global trend analysis of the aerosol optical depth using a data-assimilation grade over-water MODIS and Level 2 MISR aerosol products, *Atmos. Chem. Phys.*, *10*(22), 10,949–10,963.
- Zhu, Z., et al. (2016), Greening of the Earth and its drivers, *Nature Clim. Change, advance online publication*, *6*, 791–795, doi:10.1038/nclimate3004.